Atmos. Chem. Phys. Discuss., 15, 31053–31087, 2015
www.atmos-chem-phys-discuss.net/15/31053/2015/
doi:10.5194/acpd-15-31053-2015

Atmospheric Chemistry and Physics Discussions

Evaluation of size segregation of elemental carbon emission in Europe: influence on atmospheric long-range transportation

Y. Chen[1,2], Y. F. Cheng[2], S. Nordmann[2,3], W. Birmili[1], H. A. C. Denier van der Gon[4], N. Ma[1], R. Wolke[1], B. Wehner[1], J. Sun[1], G. Spindler[1], Q. Mu[2], U. Pöschl[2], H. Su[2], and A. Wiedensohler[1]

[1]Leibniz-Institute for Tropospheric Research, Leipzig, Germany
[2]Multiphase Chemistry Department, Max Planck Institute for Chemistry, Mainz, Germany
[3]German Environmental Agency, Dessau-Roßlau, Germany
[4]TNO, dept. Climate, Air, and sustainability, Utrecht, the Netherlands

Received: 25 September 2015 – Accepted: 19 October 2015 – Published: 6 November 2015

Correspondence to: Y. F. Cheng (yafang.cheng@mpic.de)
and A. Wiedensohler (ali@tropos.de)

Published by Copernicus Publications on behalf of the European Geosciences Union.

Abstract

Elemental Carbon (EC) has significant impact on human health and climate change. In order to evaluate the size segregation of EC emission and investigation of its influence on atmospheric transport processes in Europe, we used the fully coupled online Weather Research and Forecasting/Chemistry model (WRF-Chem) at a resolution of 2 km focusing on a region in Germany, in conjunction with a high-resolution EC emission inventory. The ground meteorology conditions, vertical structure and wind pattern were well reproduced by the model. The simulations of particle number/mass size distributions were evaluated by observations taken at the central European background site Melpitz. The fine mode aerosol was reasonably well simulated, but the coarse mode was substantially overestimated by the model. We found that it was mainly due to the nearby point source plume emitting a high amount of EC in the coarse mode. The comparisons between simulated EC and Multi-angle Absorption Photometers (MAAP) measurements at Melpitz, Leipzig-TROPOS and Bösel indicated that coarse mode EC (ECc) emission in the nearby point sources might be overestimated by a factor of 2–10. The emission fraction of EC in coarse mode was overestimated by about 10–30 % for Russian and 5–10 % for Eastern Europe (e.g.: Poland and Belarus), respectively. This overestimation in ECc emission fraction makes EC particles having less opportunity to accumulate in the atmosphere and participate to the long range transport, due to the shorter lifetime of coarse mode aerosol. The deposition concept model showed that the transported EC mass from Warsaw and Moskva to Melpitz may be reduced by 25–35 and 25–55 % respectively, due to the overestimation of ECc emission fraction. This may partly explain the underestimation of EC concentrations for Germany under eastern wind pattern in some other modelling research.

ACPD
15, 31053–31087, 2015

1 Introduction

Elemental carbon (EC) and black carbon (BC) are characterized by their strongly radiation absorbing effect (Hansen et al., 2000; Jacobson et al., 2000; Bond et al., 2013) and adverse health effects (Pope et al., 2009; Bond et al., 2013). For climate change, EC is the second strongest contributor to current global warming with a total radiative forcing of about $+1.1\,W\,m^{-2}$, just after the carbon dioxide (Bond et al., 2007; Ramanathan et al., 2008). Globally, biomass burning (40 %), fossil fuel combustion (40 %) and biofuels combustion (20 %) are the major source of EC emission (Ramanathan et al., 2008). The EC particles freshly emitted from incomplete combustion have sizes around 100 nm (Rose et al., 2006). The EC particles size information is also very significant for climate, long range transport and health effect. These fine mode EC particles are much more important than the coarse mode, since the fine EC particles have longer lifetime than coarse particles (Petzold and Kärcher, 2012; Croft et al., 2014), they have higher chances to accumulate in the atmosphere and participate long range transportation (e.g. Himalayan and arctic region), then contribute to the global scale climate forcing. Previous studies showed that EC long range transport and deposition on ice could contribute to the glacier melting in Himalayan (Ming et al., 2008) and arctic region (McConnell et al., 2007; Ramanathan et al., 2008).The EC deposition on snow and ice could change the surface albedo, absorbs solar radiation and causes positive climate forcing. Furthermore, for health effect, the fine EC particles could translocate from lung to blood with the adsorbed toxic matters (e.g.: heavy metal) inducing many disease (Pope et al., 2009; Meister et al., 2012). Global emission inventories for EC have been published (e.g.: Bond et al., 2004 and Lamarque et al., 2010). An emission inventory over Europe for EC (EUCAARI 42-Pan-European Carbonaceous aerosol inventory) has been published with a $1/8^{\circ} \times 1/16^{\circ}$ high resolution and separated size mode (PM_1, $PM_{1-2.5}$ and $PM_{2.5-10}$ (Visschedijk et al., 2008).

The emission inventory is one of the key factors for the evaluation of the EC climate effect with model (Vignati, 2010). The IPCC (IPCC, 2013) reported BC radiative forcing

ACPD
15, 31053–31087, 2015

of 0.4 (0.05–0.8), 0.2 and 0.04 (0.02–0.09) $W m^{-2}$ from fossil fuel combustion, biomass burning and deposition on snow, respectively. The uncertainties in the evaluation of BC global and regional climate effect may be due to uncertainties in BC mass concentrations, which are derived from BC emission and removal processes (Koch et al., 2009). Emissions of carbonaceous aerosols are notoriously uncertain (Denier et al., 2015). The European Environment Agency report (EEA, 2013) indicate that it was almost impossible to evaluate uncertainty overall at the EU level. The uncertainty for EC emissions is at least 50 % on global scales, and a factor of 2 to 5 on regional scale (Ramanathan et al., 2008). The uncertainty is originated not only from an instrument measurement uncertainty but also the conditions under which the emission factor measurements take place (Denier et al., 2015).

The definition of EC and BC depend on how these species were measured. BC is used for an optical determination and EC for a thermographic measurement method (Vignati et al., 2010; Nordmann et al., 2013). However, the discrepancies between EC and BC are usually disregarded, and they are interchangeable in the modelling studies (Vignati et al., 2010). Nordmann et al. (2013) showed that the EC and BC were good correlated in the German Ultrafine Aerosol Network (GUAN) sites measurements. Nordmann et al. (2013, 2014) indicate that EC in the model can be used as the best approximation of BC in modelling study.

Lots of modelling studies have been done to evaluate the EC emission and model performance in Europe. Koch et al. (2009) evaluated 17 global models and find out 13 of 17 models over-estimate EC in Europe. Stern et al. (2008) compared 5 models result with northern Germany observations, and none of the models could reproduce the high EC concentration at central Europe background station Melpitz. Genberg et al. (2013) pointed out that the EMEP MSC-W model underestimates the EC concentration at Melpitz may because the low model resolution can not represent local effects (like point source). Nordmann et al. (2014) pointed out that the EUCAARI inventory may underestimate the Eastern European EC emission by a factor of about 2, but not considering the size distribution of EC emission and its influence on transportation.

ACPD
15, 31053–31087, 2015

In this work, a high resolution WRF-Chem simulation was set up conjunction with the EUCAARI EC inventory, focusing on central Europe region. The modelling result was evaluated by the aerosol and EC/BC in-situ measurements from GUAN and HOPE-Melpitz Campaign. The EC emission fraction for coarse ($PM_{2.5-10}$) mode of the EUCAARI inventory was evaluated. The lifetime size dependent transportation concept model was designed to show the significane of size information for EC transport. The high polluted episode in 2009 April (Nordmann et al., 2014) was re-simulated for validating the influence of size segregation in EC transportation.

2 Data and method

2.1 WRF-Chem model

The fully coupled "online" Weather Research and Forecasting/Chemistry model (WRF-Chem V3.5.1) is a state-of-the-art regional air quality model (Grell et al., 2005). It is suitable for a broad spectrum of atmospheric research with horizontal extents ranging from hundreds meters to thousands kilometers. Trace gases, aerosols, and interactive processes with meteorology are simulated with several treatments in the model (Grell et al., 2005). The following is a brief summary of the primary WRF-Chem modules relevant to the current study.

2.1.1 Gas phase chemistry

In this study, the Carbon-Bond Mechanism version Z (CBMZ, Zaveri et al., 1999; Fast et al., 2006) was used for gas-phase atmospheric chemistry. 67 prognostic species and 164 reactions are included in CBMZ mechanism with a lumped structure approach, which classifies organic compounds according to their internal bond types. Fast-J scheme (Wild et al., 2000; Barnard et al., 2004) was used for calculating the rates for photolytic reactions within CBMZ.

ACPD
15, 31053–31087, 2015

2.1.2 Aerosol representation

For representing aerosol particles in WRF-Chem in this study, the MOdel for Simulating Aerosol Interactions and Chemistry (MOSAIC, Zaveri et al., 2008) is used. In MOSAIC, dry aerosol particles with eight discrete size bins were selected with upper and lower bin diameters defined as shown in Table 1; and particles are assumed to be inter-mixed in each bin (Zaveri et al., 2008).

MOSAIC treats the following chemical species: sulfate, methane sulfonate, nitrate, chloride, carbonate, ammonium, sodium, calcium, elemental carbon (EC), organic carbon (OC) and other inorganic mass. Both particle mass and particle number are simulated for each bin. Water uptake or loss will not transfer particles between bins, since bins are based on dry particle diameters (Zaveri et al., 2008). However, particle growth or reduction due to chemical processes (e.g., uptake or release of trace gases, etc.) and physical processes (e.g., coagulation, etc.) will transfer particles between bins (Chapman et al., 2009). In addition, particle coagulation and nucleation processes of sulfuric acid and water vapor are included (Fast et al., 2006; Zaveri et al., 2008). But the formation mechanism of Secondary Organic Aerosol (SOA) is not included in this version (Zaveri et al., 2008).

In WRF-Chem, dry (Binkowski et al., 1995) and wet (Easter et al., 2004) deposition processes of aerosol particles are considered. The dry deposition of aerosol in the lowest model layer is derived from the deposition velocities, which is depended on the sublayer resistance, aerodynamic resistance and surface resistance (Grell et al., 2005). The scavenging of cloud-phase and below-cloud aerosol by interception and impaction processes is calculated by look-up tables. It is worth mention that the particles are treated internally mixed in each bin; therefore the hygroscopicity of EC contained particles tends to be slightly overestimated in the model. Furthermore, the model tends to overestimate the removal rate of EC, especially for the wet deposition processes (Nordmann, 2014). In additional, Saide et al. (2012) pointed out that the irreversible removal of aerosol by rain in the WRF-Chem might make the wet deposition being

ACPD
15, 31053–31087, 2015

overestimated. However, it was mostly dry condition before 16 September 2013 in this simulation.

2.1.3 Model setup

As shown in Fig. 1, the simulation consists of 4 nested domains with 39 vertical layers. The outer domain (D01) covers Europe and the inner domain (D04) focus on Saxony in Germany with the spatial resolution of 2 km and is centered at Melpitz (12.93° E, 51.53° N). The time period from 10 to 20 September 2013 was simulated, with 2 days spin-up. The model meteorology fields are driven and forced by Final Analysis (FNL) Operational Global Analysis data (http://rda.ucar.edu/datasets/ds083.2/) and sea surface temperature (SST) dataset (http://polar.ncep.noaa.gov/sst/oper/Welcome.html) from NCEP (National Center for Environmental Prediction), with 1 ° spatial and 6 h temporal resolution. The chemical initial and boundary conditions were driven and forced by MOZART-4 global model results (http://www.acd.ucar.edu/wrf-chem/mozart.shtml) with 1.9° × 2.5° spatial and 6 h temporal resolution. The physics schemes used for simulation are summarized in Table 2. The aerosol-cloud-radiation interaction is turned on.

2.2 Emissions

In this study, biogenic emissions are taken from the Model of Emissions of Gases and Aerosols from Nature (MEGAN, Guenther et al., 2006). The Fire INventory from NCAR (FINN, Wiedinmyer et al., 2011), with 1 km spatial and 1 h temporal resolution, was used in this study. In previous studies it was shown that the dust emission scheme (Saide et al., 2012) and the sea-salt emission scheme (Saide et al., 2012; Zhang et al., 2013) in WRF-Chem have large uncertainties. However, based on the filter measurements with high volume sampler DIGITEL DHA-80 (Walter Riemer Messtechnik, Germany) at Melpitz, dust and sea-salt have contribution less than 3 % of aerosol mass in the simulation period. So, the online sea-salt and dust emissions are switched off.

ACPD
15, 31053–31087, 2015

The anthropogenic emissions were taken from the Pan-European Carbonaceous aerosol inventory (Visschedijk et al., 2008) for EC and OC, which was developed in the framework of the European Integrated project on Aerosol Cloud Climate and Air Quality interactions (EUCAARI, Kulmala et al., 2011) for the year 2005. It is available on a spatial resolution of $1/8^\circ \times 1/16^\circ$ longitude–latitude grid, corresponding to around 7 km (Fig. 1). Point source emissions are distributed according to location, capacity and fuel type (if available), and area sources are distributed using distribution maps of proxy data such as population density, detailed descriptions for gridding are given in Denier et al. (2010). The EC emissions in different size modes (PM_1, $PM_{1-2.5}$ and $PM_{2.5-10}$) are provided. The emissions are assumed to be equally distributed over the whole year. A diurnal cycle of the emissions were applied with two maxima, around 07:00 and 18:00 LT. The emissions were allocated in the first 6 layers (from surface to about 550 m) of the model depending on the emission types, such as area emission, small and large point sources. The vertical turbulent mixing was turned on in the simulation. The comparison between EUCAARI and Lamarque EC emission (Bond et al., 2007; Junker et al., 2008; Lamarque et al., 2010) was given in Nordmann et al. (2014), which shown that the EUCAARI emissions are around 30 % higher in eastern European countries Poland, Czech Republic and Belarus.

The EMEP inventory for 2013 (http://www.ceip.at, Mareckova, 2013), with $0.5^\circ \times 0.5^\circ$ spatial resolution, was applied in the model for the other anthropogenic emissions, such as PM, SO_2, NO_x, CO, NH_3, NH_4 and volatile organic compounds (VOC). The emissions of VOCs from EMEP were allocated to compounds used in CBMZ chemical mechanism of WRF-Chem.

2.3 Observations

The measurements from HOPE-Melpitz Campaign $(HD(CP)^2$ Observational Prototype Experiment, https://icdc.zmaw.de/hopm.html) and German Ultrafine Aerosol Network (GUAN, Birmili et al., 2009) are used for model evaluation. The meteorological variables (e.g. temperature, relative humidity, wind speed, wind direction), gaseous pollutants

ACPD
15, 31053–31087, 2015

(e.g. O_3, NO_x, SO_2) were simultaneously measured. In addition, the radio-sounding data for the stations all-over Europe (http://www.weather.uwyo.edu/upperair/sounding.html) were used for evaluating the modelled atmosphere vertical structure.

The regional background site Melpitz (12.93° E, 51.53° N) site is representative for a larger rural area in Saxony Germany, detailed description was given in (Brüggemann et al., 1999; Spindler et al., 2010, 2012; Poulain et al., 2011). A Twin Differential Mobility Particle Sizer (TDMPS, TROPOS, Leipzig, Germany; Birmili et al., 1999) was used to measure the Particle Number Size Distribution (PNSD) with an electrical mobility diameter between 5 and 800 nm. An Aerodynamic Particle Sizer (APS Model 3320, TSI, Inc., Shoreview, MN USA) was employed to measure PNSD with aerodynamic diameter from 0.5 to 10 µm. All of them were operated under dry conditions. All the particles were assumed as spherical (shape factor = 1), with a density of 1.8 g cm^{-3} for the submicrometer particles and 1.5 g cm^{-3} for the super-micrometer particles (Heintzenberg et al., 1998). The mobility diameter can be calculated from the aerodynamic diameter and Particle Mass Size Distribution (PMSD) can be calculated from PNSD, details were described in Heintzenberg et al. (1998). Then PNSD and PMSD in the diameter range of 5–10 000 nm can be derived from TDMPS (5–638 nm) and APS (638–10 000 nm) measurements. A high volume sampler DIGITEL DHA-80 (Walter Riemer Messtechnik, Germany), with sampling flux of about 30 m^3 h^{-1}, was used for parallel continuous daily samples of PM_{10}, detailed information was given in Spindler et al. (2013). Additionally, radio-sounding measurements were performed in Melpitz on the days 11–14, 17 and 19 September 2013.

At Melpitz, Bösel (7.94° E, 53.0° N) and Leipzig-TROPOS (12.43° E, 51.35° N), Multi-angle Absorption Photometers (MAAP Model 5012, Thermo, Inc., Waltham, MA USA) were employed to determine the particle light absorption coefficient for dry particles. All these stations are defined as rural or urban background stations. The MAAPs were measured with 10 µm cut-off inlet and the corrected mass absorption cross-section (MAC) of 5 m^2 g^{-1} was used to derive the BC mass concentration for Melpitz (Genberg et al., 2013), and the manual suggested MAC of 6.6 m^2 g^{-1} was used for Bösel and

ACPD
15, 31053–31087, 2015

Leipzig-TROPOS. Since EC and absorption-related BC are highly correlated in Germany GUAN Network sites (Nordmann et al., 2013), we use the MAAP measured BC as the best approximation of EC (Nordmann et al., 2014) in this study.

3 Result and discussion

3.1 Meteorology conditions

The WRF performance on simulating the meteorological fields was evaluated with the Melpitz ground measurements data and radio-sounding measurements over the whole Europe. The wind pattern in simulated time period was dominated by westerly winds in Melpitz (Fig. S1d in the Supplement). It is mostly in dry condition between 13 and 15 September in Melpitz. The air mass of northern Germany changed from continental to maritime after 15 September. As shown in Fig. S1 in the Supplement, the temperature, relative humidity, wind speed and wind direction were in good agreement with the measurements, with a correlation coefficient (R^2) of 0.88, 0.72, 0.74, and 0.74 respectively. The peaks in NO concentration can be reproduced by the model, although there is some overestimation (Fig. S2 in the Supplement). The transport process and emission location were also supposed to be well described in the model, because NO has very short lifetime and therefore a good indicator of nearby source. These results show that the WRF model can well reproduce the near surface meteorological condition and transport processes at Melpitz.

The vertical gradient of the potential temperature is an important indicator for the stability of atmosphere. Figure S3 in the Supplement shows a R^2 map of comparison between radio-sounding observed and simulated vertical potential temperature in planetary boundary layer (PBL, under 3 km). The R^2 are higher than 0.8 for all the stations over Europe, especially for Melpitz region the R^2 is higher than 0.9. The comparison at the Melpitz site is shown in Table 3, together with some profile examples in Fig. S4 in the Supplement. The modelled meteorological vertical structure was in good agree-

ACPD
15, 31053–31087, 2015

ment with measurements, with R^2 value of 0.98, 0.84, 0.93 and 0.70 for the potential temperature, water vapor mixing ratio, wind speed and wind direction respectively. The results indicate that WRF well simulated the meteorological vertical structure and wind pattern, especially in central Europe (Melpitz region with 2 km resolution).

3.2 Particle size distribution

The modelled particle number size distribution (PNSD) and particle mass size distribution (PMSD) for Melpitz were compared with the measurements, shown in Fig. 2. For the fine mode (PM_1) aerosol the agreement is acceptable, but the model significantly overestimated the coarse mode ($PM_{2.5-10}$) mass/number. The meteorology condition was well reproduced by the model. The transportation process was also supposed to be well simulated. It indicates that there may be some unrealistic sources of particles larger than 2.5 µm included in the model, which leads to the overestimation of coarse mode.

We found out that EC has a very high contribution of modelled coarse mode aerosol mass when the EC plumes hit Melpitz (Figs. 3a and 4a). In order to investigate the reasons of the EC plumes and its influence on coarse mode overestimation, a more detailed case study for the plume episode in the morning of 13 September will be given in Sect. 3.3.

3.3 Elemental Carbon source evaluation

In order to evaluate the EC emission in central Europe and investigate local effect of point source, MAAP measurements of 3 background sites (Melpitz, Leipzig-TROPOS and Bösel) were compared with modelled result (Fig. 3). According to modelled transportations, Melpitz and Bösel were influenced by the point source plume, but Leipzig-TROPOS was not (see Fig. S5 in the Supplement). Here we use MAAP instead of DIGITEL measurement to compare with the model output, because only MAAP data

ACPD
15, 31053–31087, 2015

are available for all those three sites and the higher temporal resolution of the MAAP is better for investigating the point source plume influence.

The model substantially overestimated the EC concentration in Melpitz especially for high episode peaks (Fig. 3a), during which the modelled EC concentration in PM_{10} can reach up to about 3–4 times higher than that in $PM_{2.5}$, while the average ratio between EC concentration in PM_{10} and $PM_{2.5}$ is only 150 %. Comparing with MAAP measurement, EC in PM_{10} was on average overestimated by a factor of 2.8 at Melpitz, and by a factor up to 6–10 for the peak periods. This overestimation of EC by model is due to the plume from a point source emission of type SNAP-5 (extraction and distribution fossil fuels, nomenclature described in Visschedijk et al., 2008 and Pouliot et al., 2012) located between Leipzig and Melpitz. Figure 4 is an example snapshot showing the EC plume passing through Melpitz at 05:00 a.m. on 13 September 2013. Plumes from the same sources also similarly influenced other peak periods to different extend. When the plume hitting Melpitz, the overestimation of EC concentration was substantial even when the uncertainties in the modelled transportation within 12 km × 12 km was accounted for (shaded area in Fig. 3a), and EC contributed 30–67 % of coarse mode aerosol mass. At the same time, Leipzig was not influenced by point source plume, because of the prevailing westerly wind in domain D04 (Fig. 4b). The comparison at the Leipzig-TROPOS site is thus much better (Fig. 3b). There, EC is only slightly overestimated by less than 40 %, which may be due to the seasonal variability and/or reducing emissions (~ 25 % from 2010 to 2013, based on long term MAAP measurements in Leipzig-TROPOS and DIGITEL measurements in Melpitz) in context of Saxony "low emission zone" policy since March 2011 (http://gis.uba.de/website/umweltzonen/umweltzonen_en.php). The different behaviors of model at these two sites indicate that the coarse mode EC emission in the point sources near Melpitz can be significantly overestimated.

This EC plume effect was not only found in Melpitz. As shown in Fig. S5 in the Supplement, Bösel was also influenced by a nearby EC point source in the morning of 13 and 14 September 2013 (also Fig. 3c). The EC concentration was overestimated

ACPD
15, 31053–31087, 2015

and had a high coarse mode fraction, similar to Melpitz. However, the overestimation of EC was not as significant as for Melpitz, with ~ 87 % on average and about 200–400 % during the peak periods. The fraction of EC in coarse mode was also not as high as in Melpitz. One reason could be the lower intensity of the point source nearby Bösel than the one near Melpitz (Fig. S5 in the Supplement). Another reason may be the artificial dilution of local emissions by the coarser modelling resolution (Genberg et al., 2013), because we only have the highest resolution of 2 km covering the regions around Melpitz (D04), but 6 km resolution for Bösel (D03).

These results imply that the EC point sources in Germany can be overestimated by a factor of 2–10 in the EUCAARI emission inventory, especially for the coarse mode EC emission in the large point sources. To further evaluate the coarse mode EC emission (ECc, EC in $PM_{2.5-10}$) over the whole Europe, we first checked the emission fraction of ECc to the total EC in EUCAARI inventory. As shown in Fig. 5, this fraction for the sum of area and point sources is generally lower than 10 % over large regions in Western Europe. For almost all of the point sources, the ECc emission fractions are higher than 30 % (Fig. S6 in the Supplement), within which there are 3 and 10 point sources around Melpiz and Bösel region, respectively, with ECc emission fractions even higher than 80 % (Table S1 and Fig. S6 in the Supplement). It is worth mentioning that these point sources with high ECc emission fractions also have a very high total EC emission rate. For example, the point source, influencing Melpitz in the morning of 13 September, is the largest point source for SNAP-5 in Germany with a share of about 20 % in the total EC point emission. EC emissions from the SNAP-5 point sources are originated from coal-mining, storage and handling (Visschedijk et al., 2008; Pouliot et al., 2012; Denier et al., 2015), for which a relatively high fraction in coarse mode emission is expected. Therefore, the emission fraction of ECc may be true. But, the total EC emission rate might be too high due to the overestimation of EC scaling factor out of all emitted compounds. But it is hard to quantify it due to the fact that little data are available for the storage and handling of coal, and about chemical composition and size distribution of the emission in SNAP-5 type of emissions.

ACPD
15, 31053–31087, 2015

3.4 Influence on atmospheric transportation

EC is in general mostly emitted in the fine mode, especially for the area emissions (Echalar et al., 1998; Hitzenberger et al., 2001; Kuenen et al., 2014). Based on the EUCAARI inventory, the average ECc emission fraction for Western Europe is around 5 %, consistent with previous knowledge. But on the contrast to the generally low ECc emission fraction, this fraction is relatively high in Eastern Europe (e.g. Poland, Slovakia and Belarus) of about 15–20 %. For Russia (including Kaliningrad in the north of Poland) and Moldova the fraction can reach up to 20–40 %. As shown in the long-term (2003–2011) filter measurement study at Melpitz (Spindler et al., 2013), in the eastern wind dominated period when the air mass came from Eastern Europe and Russia, the EC coarse mode mass fraction was only in the range of 4–15 % (~ 10 % in average). Assuming that EC particles would not change the size during transportation, EUCAARI inventory may overestimate the fraction of ECc about 5–10 % for Eastern Europe and 10–30 % for Russian.

The life-time for fine mode particles is about 5–7 days, but only 1–2 days for the coarse mode aerosol (Jaenicke et al., 1980; Petzold and Kärcher, 2012; Croft et al., 2014). Therefore, the fine mode EC have more time to accumulate in the atmosphere. To evaluate the influence of this high coarse mode EC emission fraction in Eastern Europe on EC's long-range transportation, we constructed the following concept model. In a steady state, where aerosol sources are continuous and there is a quasi-equilibrium between sources and sinks such that the EC concentration is constant in time. For the same emission rate of EC, the equilibrium mass concentration of fine mode will be 2–3 times higher than coarse mode as described in Eq. (1) (Croft et al., 2014). The deposition rate of EC in coarse mode is also 2–3 times higher than in fine mode, as described in Eq. (2).

$$\frac{\mathrm{d}C(t)}{\mathrm{d}t} = S(t) - \frac{C(t)}{\tau(t)} \quad (1)$$

ACPD
15, 31053–31087, 2015

where $C(t)$ is the EC concentration at time t, $S(t)$ is the source rate, and $\tau(t)$ is the removal timescale. In the steady state, a quasi-equilibrium between sources and sinks, $\tau(t)$ is defined as lifetime (Croft et al., 2014). Then the deposition rate (sink rate, Ar), with unit of percentage per second, can be defined as:

$$\mathrm{Ar} = \frac{\mathrm{As}}{C} = \frac{1}{\tau} \quad (2)$$

Where As is the deposition speed, C is the steady state EC concentration, and τ is the steady state lifetime.

On the other hand, longer lifetime makes fine mode EC having more opportunity to be transported from Eastern Europe to Melpitz. In the following scenario, the particles were emitted instantly into the air mass, which was assumed to be transported by an eastern wind pattern with $5\,\mathrm{m\,s^{-1}}$ speed. It will take about 4–5 days from Moskva to Melpitz, and 1–2 days from Warsaw Poland. During the transport, only the deposition process was active and described as Eq. (2), without subsequent emission. About 30–55 % and 65–85 % of fine mode EC can be transported to Melpitz from Moskva and Warsaw Poland respectively, but just 5–20 and 10–60 % for the coarse mode EC can make the same way (Fig. 6).

The overestimation of ECc emission fraction in EUCAARI inventory make less EC could be transported from the Eastern Europe and Russia to Melpitz. This may be one reason of the underestimation of the EC mass concentration in the other studies under eastern wind pattern (Stern et al., 2008; Genberg et al., 2013; Nordmann et al., 2014).

Nordmann et al. (2014) reported an underestimation of EC about 50 % during March–April 2009 in Germany, especially for the period when air mass approached the observation sites from eastern directions. And they suspected that the EC emission in Eastern Europe may be underestimated by a factor of 2 to 5. In order to investigate the possible influence of the overestimated coarse mode EC emission fraction in Eastern Europe in this case, we re-simulated the same time period as in Nordmann et al. (2014) with the adjusted EC emission inventory. The ECc emission fraction was adjusted to 5 % (the average value for Western Europe, longitude < 15° E) if it is higher

ACPD
15, 31053–31087, 2015

than 5 % in Eastern Europe (longitude > 15° E). The new simulation and the results of Nordmann et al. (2014) are shown in Table 4. The air mass origin for the high EC concentration period (4 April 2009, Nordmann et al., 2014) is shown by back trajectories in Fig. 5. The back trajectories were calculated based on the GDAS (with 0.5° resolution) dataset with the Hysplit model (http://www.arl.noaa.gov/HYSPLIT_info.php). The underestimation for EC was significantly improved for Bösel and Leipzig-TROPOS. For Bösel, the mean normalized bias (MNB) increased from −21 to 13 % and R^2 from 0.61 to 0.81; for Leipzig-TROPOS, the MNB increased from −70 to −47 % and R^2 from 0.35 to 0.69. The results for Hohenpeißenberg and Zugspitze were not significantly changed, with differences in MNB less than 10 %. This is because the air masses for Bösel and Leipzig-TROPOS were from Eastern Europe passing through Poland, where the ECc emission fraction in EUCAARI inventory is high. But it was not the case for Southeast Europe, where the air mass for Hohenpeißenberg and Zugspitze originated from (Fig. 5). Thus, it indicate that the Nordmann et al. (2014)'s conclusion of underestimation of EC emission in eastern Europe for 2009 is generally correct, especially for Southeastern Europe (e.g.: Austria, Slovenia, Croatia etc.). However, the overestimation of the ECc emission fraction in Eastern Europe (e.g.: Poland, Belarus, Russian etc.) could be another reason for the underestimation of modeled EC mass concentration in the eastern wind pattern, which contributed to the EC concentration underestimation bias about 20–40 %. This is consistent with the result of concept model, which showed the adjustment of ECc emission fraction in Warsaw Poland would make about 25–55 % difference of EC transported to Melpitz.

4 Conclusions

The main goals of this study are the evaluation for EC emission in Europe, including size segregation and point sources. The corresponding influences on transport and plume effect are also investigated. A WRF-Chem simulation was performed for the period between 10 and 20 September 2013, with an inner most domain of 2 km resolution

ACPD
15, 31053–31087, 2015

for the Melpitz region in eastern Germany. The high resolution EUCAARI inventory of EC emission was applied in the model. The measurements of HOPE-Melpitz Campaign and GUAN network project were used for modelling results validation.

The comparison of particle number/mass size distributions showed that the coarse mode aerosol was substantially overestimated by the model. However, the meteorology and transport process were well simulated, because of the good agreement with the ground-based and radio-sounding meteorological measurements. These results indicated that overestimation of the coarse mode aerosol should mostly come from the uncertainty of emission inventories. The comparisons of EC mass concentrations in Melpitz, Leipzig-TROPOS and Bösel indicated that the EC point sources may be overestimated by a factor of 2–10, which made a remarkable unrealistic plume in Melpitz.

The coarse mode EC emission fraction was substantially overestimated for Eastern Europe (e.g.: Poland, Belarus etc.) and Russia in EUCAARI inventory, with about 10–30 % for Russia and 5–10 % for the Eastern Europe countries. A concept model was designed to interpret the influence of this overestimation on EC long range transportation. Due to the overestimation of ECc emission fraction, EC mass transported from Moskva to Melpitz would decrease about 25–35 % of ECc mass concentration, and decrease about 25–55 % from Warsaw to Melpitz. This is because the coarse mode aerosol has a shorter life-time and therefore less opportunity for being long range transported and accumulated in the atmosphere. The March–April 2009 case (Nordmann et al., 2014) was re-simulated with adjusted ECc emission fraction in Eastern Europe in order to validate the influence on transportation. The result showed that the overestimation of ECc emission fraction in Eastern Europe was one reason of the underestimation of EC in Germany, when the air masses came from eastern direction. It contributed to an underestimation of about 20–40 %.

Will the health and climatic effects of atmospheric EC particles be local, regional or global? This is some extent determined by the transportation of EC, which is largely influenced by its size distribution. The size segregation information of EC particles should be carefully considered in the model validation and climate change evaluation studies.

ACPD
15, 31053–31087, 2015

Unfortunately, the size segregation information is not included in most of current EC emission inventories, and the size segregation in EUCAARI inventory only covers Europe and is still with high uncertainty. More EC particle size distribution measurements (e.g.: online analysis of SP2, offline analysis of Berner/MOUDI samples, etc.) and long term model simulation studies are needed to further improve the EC emission inventories.

The Supplement related to this article is available online at doi:10.5194/acpd-15-31053-2015-supplement.

Acknowledgements. Continuous aerosol measurements at Melpitz were supported by the German Federal Environment Ministry (BMU) grants F&E 370 343 200 (German title: "Erfassung der Zahl feiner und ultrafeiner Partikel in der Außenluft") and F&E 371 143 232 (German title: "Trendanalysen gesundheitsgefährdender Fein- und Ultrafeinstaubfraktionen unter Nutzung der im German Ultrafine Aerosol Network (GUAN) ermittelten Immissionsdaten durch Fortführung und Interpretation der Messreihen"). The HOPE campaign was funded by the German Research Ministry under the project number 01LK1212 C. We would also like to thank Markus Hermann and Sascha Pfeifer for useful suggestions.

References

Barnard, J. C., Chapman, E. G., Fast, J. D., Schemlzer, J. R., Slusser, J. R., and Shetter, R. E.: An evaluation of the FAST-J Photolysis Algorithm for predicting nitrogen dioxide photolysis rates under clear and cloudy sky conditions, Atmos. Environ., 38, 3393–3403, 2004.

Binkowski, F. S. and Shankar, U.: The Regional Particulate Matter Model: 1. Model description and preliminary results, J. Geophys. Res., 100, 26191–26209, doi:10.1029/95JD02093, 1995.

Birmili, W., Stratmann, F., and Wiedensohler, A.: Design of a DMAbased size spectrometer for a large particle size range and stable operation, J. Aerosol Sci., 30, 549–533, 1999.

ACPD
15, 31053–31087, 2015

Birmili, W., Weinhold, K., Nordmann, S., Wiedensohler, A., Spindler, G., Müller K., Herrmann, H., Gnauk, T., Pitz, M., Cyrys, J., Flentje, H., Nickel, C., Kuhlbusch, T., Löschau G., Haase, D., Meinhardt, F., Schwerin, A., Ries, L., and Wirtz, K.: Atmospheric aerosol measurements in the German Ultrafine Aerosol Network (GUAN) – Part – soot and particle number size distributions, Gefahrst. Reinhalt. L., 69, 137–145, 2009.

Bond, T. C., Streets, D. G., Yarber, K. F., Nelson, S. M., Woo, J., and Klimont, Z.: A technology-based global inventory of black and organic carbon emissions from combustion, J. Geophys. Res., 109, D14203, doi:10.1029/2003JD003697, 2004.

Bond, T. C., Bhardwaj, E., Dong, R., Jogani, R., Jung, S., Roden, C., Streets, D. G., and Trautmann, N. M.: Historical emissions of black and organic carbon aerosol from energy-related combustion, 1850–2000, Global Biogeochem. Cy., 21, GB2018, doi:10.1029/2006GB002840, 2007.

Bond, T. C., Doherty, S. J., Fahey, D. W., Forster, P. M., Berntsen, T., DeAngelo, B. J., Flanner, M. G., Ghan, S., Kärcher, B., Koch, D., Kinne, S., Kondo, Y., Quinn, P. K., Sarofim, M. C., Schultz, M. G., Schulz, M., Venkataraman, C., Zhang, H., Zhang, S., Bellouin, N., Guttikunda, S. K., Hopke, P. K., Jacobson, M. Z., Kaiser, J. W., Klimont, Z., Lohmann, U., Schwarz, J. P., Shindell, D., Storelvmo, T., Warren, S. G., and Zender, C. S.: Bounding the role of black carbon in the climate system: a scientific assessment, J. Geophys. Res.-Atmos., 118, 5380–5552, doi:10.1002/jgrd.50171, 2013.

Brüggemann E. and Spindler, G.: Wet and dry deposition of sulphur at the site Melpitz in East Germany, Water Air Soil Poll., 109, 81–99, 1999.

Chapman, E. G., Gustafson Jr., W. I., Easter, R. C., Barnard, J. C., Ghan, S. J., Pekour, M. S., and Fast, J. D.: Coupling aerosol-cloud-radiative processes in the WRF-Chem model: Investigating the radiative impact of elevated point sources, Atmos. Chem. Phys., 9, 945–964, doi:10.5194/acp-9-945-2009, 2009.

Croft, B., Pierce, J. R., and Martin, R. V.: Interpreting aerosol lifetimes using the GEOS-Chem model and constraints from radionuclide measurements, Atmos. Chem. Phys., 14, 4313–4325, doi:10.5194/acp-14-4313-2014, 2014.

Denier van der Gon, H. A. C., Visschedijk, A., Van der Brugh, H., and Dröge, R.: A High Resolution European Emission Database for the Year 2005, a Contribution to the UBAproject PAREST: Particle Reduction Strategies, TNO report TNO-034-UT-2010-01895_RPTML, published by the German Federal Environment Agency (Umweltbundesamt) as Texte 41/2013, Utrecht, available at: https://www.umweltbundesamt.de/publikationen, 2010.

ACPD
15, 31053–31087, 2015

Denier van der Gon, H. A. C., Bergström, R., Fountoukis, C., Johansson, C., Pandis, S. N., Simpson, D., and Visschedijk, A. J. H.: Particulate emissions from residential wood combustion in Europe – revised estimates and an evaluation, Atmos. Chem. Phys., 15, 6503–6519, doi:10.5194/acp-15-6503-2015, 2015.

Easter, R. C., Ghan, S. J., Zhang, Y., Saylor, R. D., Chapman, E. G., Laulainen, N. S., Abdul-Razzak, H., Leung, L. R., Bian, X., and Zaveri, R. A.: MIRAGE: model description and evaluation of aerosols and trace gases, J. Geophys. Res., 109, D20210, doi:10.1029/2004JD004571, 2004.

Echalar, F., Artaxo, P., Martins, J. V., Yamasoe, M., Gerab, F., Maenhaut, W., and Holben, B.: Long-term monitoring of atmospheric aerosols in the Amazon Basin: source identification and apportionment, J. Geophys. Res.-Atmos., 103, 31849–31864, 1998.

EEA: (European Environment Agency): European Union Emission Inventory Report 1990–2011 Under the UNECE Convention on Long-range Transboundary Air Pollution (LRTAP), EEA Technical report No. 10/2013, Copenhagen, doi:10.2800/44480, 2013.

Fast, J. D., Gustafson Jr., W. I., Easter, R. C., Zaveri, R. A., Barnard, J. C., Chapman, E. G., Grell, G. A., and Peckham, S. E.: Evolution of ozone, particulates, and aerosol direct radiative forcing in the vicinity of Houston using a fully coupled meteorology-chemistry-aerosol model, J. Geophys. Res., 111, D21305, doi:10.1029/2005JD006721, 2006.

Genberg, J., Denier van der Gon, H. A. C., Simpson, D., Swietlicki, E., Areskoug, H., Beddows, D., Ceburnis, D., Fiebig, M., Hansson, H. C., Harrison, R. M., Jennings, S. G., Saarikoski, S., Spindler, G., Visschedijk, A. J. H., Wiedensohler, A., Yttri, K. E., and Bergström, R.: Light-absorbing carbon in Europe – measurement and modelling, with a focus on residential wood combustion emissions, Atmos. Chem. Phys., 13, 8719–8738, doi:10.5194/acp-13-8719-2013, 2013.

Grell, G. A., Peckham, S. E., Schmitz, R., McKeen, S. A., Frost, G., Skamarock, W. C., and Eder, B.:: Fully coupled "online" chemistry within the WRF model, Atmos. Environ., 39, 6957–6975, 2005.

Guenther, A., Karl, T., Harley, P., Wiedinmyer, C., Palmer, P. I., and Geron, C.: Estimates of global terrestrial isoprene emissions using MEGAN (Model of Emissions of Gases and Aerosols from Nature), Atmos. Chem. Phys., 6, 3181–3210, doi:10.5194/acp-6-3181-2006, 2006.

Hansen, J. E., Sato, M., Ruedy, R., Lacis, A., and Oinas, V.: Global warming in the twenty-first century: an alternative scenario, P. Natl. Acad. Sci. USA, 97, 9875–9880, 2000.

ACPD
15, 31053–31087, 2015

Heintzenberg, J., Müller, K., Birmili, W., Spindler, G., and Wiedensohler, A.: Mass-related aerosol properties over the Leipzig Basin, J. Geophys. Res.-Atmos., 103, 13125–13135, 1998.

Hitzenberger. R. and Tohno, S.: Comparison of black carbon (BC) aerosols in two urban areas – concentrations and size distributions, Atmos. Environ., 35, 2153–2167, 2001.

IPCC A R.: Climate Change 2013: The Physical Science Basis, Contribution of Working Group I to the Fifth Assessment Report of the Intergovernmental Panel on Climate Change, Report, Cambridge University Press, New York, 2013.

Jacobson, M. Z.: A physically-based treatment of elemental carbon optics: implications for global direct forcing of aerosols, Geophys. Res. Lett., 27, 217–220, doi:10.1029/1999GL010968, 2000.

Jaenicke, R.: Atmospheric aerosols and global climate, J. Aerosol Sci., 11, 577–588, 1980.

Junker, C. and Liousse, C.: A global emission inventory of carbonaceous aerosol from historic records of fossil fuel and biofuel consumption for the period 1860–1997, Atmos. Chem. Phys., 8, 1195–1207, doi:10.5194/acp-8-1195-2008, 2008.

Koch, D., Schulz, M., Kinne, S., McNaughton, C., Spackman, J. R., Balkanski, Y., Bauer, S., Berntsen, T., Bond, T. C., Boucher, O., Chin, M., Clarke, A., De Luca, N., Dentener, F., Diehl, T., Dubovik, O., Easter, R., Fahey, D. W., Feichter, J., Fillmore, D., Freitag, S., Ghan, S., Ginoux, P., Gong, S., Horowitz, L., Iversen, T., Kirkevåg, A., Klimont, Z., Kondo, Y., Krol, M., Liu, X., Miller, R., Montanaro, V., Moteki, N., Myhre, G., Penner, J. E., Perlwitz, J., Pitari, G., Reddy, S., Sahu, L., Sakamoto, H., Schuster, G., Schwarz, J. P., Seland, Ø., Stier, P., Takegawa, N., Takemura, T., Textor, C., van Aardenne, J. A., and Zhao, Y.: Evaluation of black carbon estimations in global aerosol models, Atmos. Chem. Phys., 9, 9001–9026, doi:10.5194/acp-9-9001-2009, 2009.

Kuenen, J. J. P., Visschedijk, A. J. H., Jozwicka, M., and Denier van der Gon, H. A. C.: TNO-MACC_II emission inventory; a multi-year (2003–2009) consistent high-resolution European emission inventory for air quality modelling, Atmos. Chem. Phys., 14, 10963–10976, doi:10.5194/acp-14-10963-2014, 2014.

Kulmala, M., Asmi, A., Lappalainen, H. K., Baltensperger, U., Brenguier, J.-L., Facchini, M. C., Hansson, H.-C., Hov, Ø., O'Dowd, C. D., Pöschl, U., Wiedensohler, A., Boers, R., Boucher, O., de Leeuw, G., Denier van der Gon, H. A. C., Feichter, J., Krejci, R., Laj, P., Lihavainen, H., Lohmann, U., McFiggans, G., Mentel, T., Pilinis, C., Riipinen, I., Schulz, M., Stohl, A., Swietlicki, E., Vignati, E., Alves, C., Amann, M., Ammann, M., Arabas, S., Artaxo, P., Baars, H.,

ACPD
15, 31053–31087, 2015

Beddows, D. C. S., Bergström, R., Beukes, J. P., Bilde, M., Burkhart, J. F., Canonaco, F., Clegg, S. L., Coe, H., Crumeyrolle, S., D'Anna, B., Decesari, S., Gilardoni, S., Fischer, M., Fjaeraa, A. M., Fountoukis, C., George, C., Gomes, L., Halloran, P., Hamburger, T., Harrison, R. M., Herrmann, H., Hoffmann, T., Hoose, C., Hu, M., Hyvärinen, A., Hõrrak, U., Iinuma, Y., Iversen, T., Josipovic, M., Kanakidou, M., Kiendler-Scharr, A., Kirkevåg, A., Kiss, G., Klimont, Z., Kolmonen, P., Komppula, M., Kristjánsson, J.-E., Laakso, L., Laaksonen, A., Labonnote, L., Lanz, V. A., Lehtinen, K. E. J., Rizzo, L. V., Makkonen, R., Manninen, H. E., McMeeking, G., Merikanto, J., Minikin, A., Mirme, S., Morgan, W. T., Nemitz, E., O'Donnell, D., Panwar, T. S., Pawlowska, H., Petzold, A., Pienaar, J. J., Pio, C., Plass-Duelmer, C., Prévôt, A. S. H., Pryor, S., Reddington, C. L., Roberts, G., Rosenfeld, D., Schwarz, J., Seland, Ø., Sellegri, K., Shen, X. J., Shiraiwa, M., Siebert, H., Sierau, B., Simpson, D., Sun, J. Y., Topping, D., Tunved, P., Vaattovaara, P., Vakkari, V., Veefkind, J. P., Visschedijk, A., Vuollekoski, H., Vuolo, R., Wehner, B., Wildt, J., Woodward, S., Worsnop, D. R., van Zadelhoff, G.-J., Zardini, A. A., Zhang, K., van Zyl, P. G., Kerminen, V.-M., S Carslaw, K., and Pandis, S. N.: General overview: European Integrated project on Aerosol Cloud Climate and Air Quality interactions (EUCAARI) – integrating aerosol research from nano to global scales, Atmos. Chem. Phys., 11, 13061–13143, doi:10.5194/acp-11-13061-2011, 2011.

Lamarque, J.-F., Bond, T. C., Eyring, V., Granier, C., Heil, A., Klimont, Z., Lee, D., Liousse, C., Mieville, A., Owen, B., Schultz, M. G., Shindell, D., Smith, S. J., Stehfest, E., Van Aardenne, J., Cooper, O. R., Kainuma, M., Mahowald, N., McConnell, J. R., Naik, V., Riahi, K., and van Vuuren, D. P.: Historical (1850–2000) gridded anthropogenic and biomass burning emissions of reactive gases and aerosols: methodology and application, Atmos. Chem. Phys., 10, 7017–7039, doi:10.5194/acp-10-7017-2010, 2010.

Mareckova, K., Wankmueller, R., Moosmann, L., and Pinterits, M.: Inventory Review 2013: Review of Emission Data reported under the LRTAP Convention and NEC Directive, Stage 1 and 2 review, Status of Gridded Data and LPS Data, STATUS Report 1/2013, Umweltbundesamt GmbH, Vienna, Austria, 2013.

McConnell, J. R., Edwards, R., Kok, G. L., Flanner, M. G., Zender, C. S., Saltzman, E. S., Banta, J. R., Pasteris, D. R., Carter, M. M., and Kahl, J. D. W.: 20th-century industrial black carbon emissions altered arctic climate forcing, Science, 317, 1381–1384, 2007.

Meister, K., Johansson, C., and Forsberg, B.: Estimated short-term effects of coarse particles on daily mortality in Stockholm, Sweden, Environ. Health Persp., 120, 431–436, 2012.

ACPD
15, 31053–31087, 2015

Ming, J., Cachier, H., Xiao, C., Qin, D., Kang, S., Hou, S., and Xu, J.: Black carbon record based on a shallow Himalayan ice core and its climatic implications, Atmos. Chem. Phys., 8, 1343–1352, doi:10.5194/acp-8-1343-2008, 2008.

Nordmann, S., Birmili, W., Weinhold, K., Müller, K., Spindler, G., and Wiedensohler, A.: Measurements of the mass absorption cross section of atmospheric soot particles using Raman spectroscopy, J. Geophys. Res.-Atmos., 118, 12075–12085, doi:10.1002/2013JD020021, 2013.

Nordmann, S., Cheng, Y. F., Carmichael, G. R., Yu, M., Denier van der Gon, H. A. C., Zhang, Q., Saide, P. E., Pöschl, U., Su, H., Birmili, W., and Wiedensohler, A.: Atmospheric black carbon and warming effects influenced by the source and absorption enhancement in central Europe, Atmos. Chem. Phys., 14, 12683–12699, doi:10.5194/acp-14-12683-2014, 2014.

Petzold, A. and Kärcher, B.: Aerosols in the Atmosphere, in: Atmospheric Physics, edited by: Schumann, U., Research Topics in Aerospace, Springer Berlin Heidelberg, 37–53, doi:10.1007/978-3-642-30183-4_3, 2012.

Pouliot, G., Pierce, T., van der Gon, H., Schaap, M., Moran, M., and Nopmongcol, U.:: Comparing emission inventories and model-ready emission datasets between Europe and North America for the AQMEII project, Atmos. Environ., 53, 4–14, 2012.

Pope, C. A., Ezzati, M., and Dockery, D. W.: Fine-particulate air pollution and life expectancy in the united states, N. Engl. J. Med., 360, 376–386, 2009.

Poulain, L., Spindler, G., Birmili, W., Plass-Dülmer, C., Wiedensohler, A., and Herrmann, H.: Seasonal and diurnal variations of particulate nitrate and organic matter at the IfT research station Melpitz, Atmos. Chem. Phys., 11, 12579–12599, doi:10.5194/acp-11-12579-2011, 2011.

Ramanathan, V. and Carmichael, G.: Global and regional climate changes due to black carbon, Nat. Geosci., 1, 221–227, 2008.

Rose, D., Wehner, B., Ketzel, M., Engler, C., Voigtländer, J., Tuch, T., and Wiedensohler, A.: Atmospheric number size distributions of soot particles and estimation of emission factors, Atmos. Chem. Phys., 6, 1021–1031, doi:10.5194/acp-6-1021-2006, 2006.

Saide, P. E., Spak, S. N., Carmichael, G. R., Mena-Carrasco, M. A., Yang, Q., Howell, S., Leon, D. C., Snider, J. R., Bandy, A. R., Collett, J. L., Benedict, K. B., de Szoeke, S. P., Hawkins, L. N., Allen, G., Crawford, I., Crosier, J., and Springston, S. R.: Evaluating WRF-Chem aerosol indirect effects in Southeast Pacific marine stratocumulus during VOCALS-REx, Atmos. Chem. Phys., 12, 3045–3064, doi:10.5194/acp-12-3045-2012, 2012.

ACPD
15, 31053–31087, 2015

Spindler, G., Brüggemann E., Gnauk, T., Grüner A., Müller K., and Herrmann, H.: A four-year size-segregated characterization study of particles PM_{10}, $PM_{2.5}$ and PM_1 depending on air mass origin at Melpitz, Atmos. Environ., 44, 164–173, 2010.

Spindler, G., Gnauk, T., Grüner, A., Iinuma, Y., Müller, K., Scheinhardt, S., and Herrmann, H.: Size-segregated characterization of PM_{10} at the EMEP site Melpitz (Germany) using a five-stage impactor: a 6 year study, J. Atmos. Chem., 69, 127–157, 2012.

Spindler, G., Grüner, A., Müller, K., Schlimper, S., and Herrmann, H.: Long-term size-segregated particle (PM_{10}, $PM_{2.5}$, PM_1) characterization study at Melpitz – influence of air mass inflow, weather conditions and season, J. Atmos. Chem., 70, 165–195, doi:10.1007/s10874-013-9263-8, 2013.

Stern, R., Builtjes, P., Schaap, M., Timmermans, R., Vautard, R., Hodzic, A., Memmesheimer, M., Feldmann, H., Renner, E., Wolke, R., and Kerschbaumer: a model inter-comparison study focussing on episodes with elevated PM_{10} concentrations, Atmos. Environ., 42, 4567–4588, doi:10.1016/j.atmosenv.2008.01.068, 2008.

Vignati, E., Karl, M., Krol, M., Wilson, J., Stier, P., and Cavalli, F.: Sources of uncertainties in modelling black carbon at the global scale, Atmos. Chem. Phys., 10, 2595–2611, doi:10.5194/acp-10-2595-2010, 2010.

Visschedijk, A. and Denier van der Gon, H.: EUCAARI Deliverable: Pan-European Carbonaceous Aerosol Inventory, Report, TNO Built Environment and Geosciences, D42, Utrecht, the Netherlands, 2008.

Wiedinmyer, C., Akagi, S. K., Yokelson, R. J., Emmons, L. K., Al-Saadi, J. A., Orlando, J. J., and Soja, A. J.: The Fire INventory from NCAR (FINN): a high resolution global model to estimate the emissions from open burning, Geosci. Model Dev., 4, 625–641, doi:10.5194/gmd-4-625-2011, 2011.

Wild, O., Zhu, X., and Prather, M. J.: Fast-J: accurate simulation of in- and below-cloud photolysis in tropospheric chemical models, J. Atmos. Chem., 37, 245–282, 2000.

Zhang, Y., Sartelet, K., Zhu, S., Wang, W., Wu, S.-Y., Zhang, X., Wang, K., Tran, P., Seigneur, C., and Wang, Z.-F.: Application of WRF/Chem-MADRID and WRF/Polyphemus in Europe – Part 2: Evaluation of chemical concentrations and sensitivity simulations, Atmos. Chem. Phys., 13, 6845–6875, doi:10.5194/acp-13-6845-2013, 2013.

Zaveri, R. A. and Peters, L. K.: A new lumped structure photochemical mechanism for large-scale applications, J. Geophys. Res., 104, 30387–30415, 1999.

ACPD
15, 31053–31087, 2015

Zaveri, R. A., Easter, R. C., Fast, J. D., and Peters, L. K.: Model for Simulating Aerosol Interactions and Chemistry (MOSAIC), J. Geophys. Res., 113, D13204, doi:10.1029/2007JD008782, 2008.

ACPD
15, 31053–31087, 2015

Table 1. Sectional approach for aerosols: particle dry-diameter ranges used in this study.

	Bin 01	Bin 02	Bin 03	Bin 04	Bin 05	Bin 06	Bin 07	Bin 08
Minimum Diameter (μm)	0.0390625	0.078125	0.15625	0.3125	0.625	1.25	2.5	5.0
Maximum Diameter (μm)	0.078125	0.15625	0.3125	0.625	1.25	2.5	5.0	10.0

ACPD
15, 31053–31087, 2015

Table 2. Configurations of WRF-Chem.

Physics	WRF option
Micro physics	Lin et. al. (1983) scheme
Surface	Rapid Update Cycle (RUC) land surface model
Boundary layer	YSU (Hong et. al., 2006)
Cumulus	Grell 3-D
Urban	3-category UCM
Shortwave radiation	Goddard shortwave (Chou et. al., 1998)
Longwave radiation	New Goddard scheme
Chemistry and Aerosol	**Chem option**
Gas-phase mechanism	CBMZ
Aerosol module	MOSAIC with 8 bins
Photolytic rate	Fast-J photolysis scheme

ACPD
15, 31053–31087, 2015

Table 3. Comparison result for meteorological variables between Melpitz radio-sounding measurements and WRF-Chem model.

	Slope	R^2	Data point Number
Potential Temperature	0.99	0.98	586
Water Vapor Mixing Ratio	0.81	0.84	586
Wind Speed	0.90	0.93	586
Wind Direction	1.02	0.70	586

ACPD
15, 31053–31087, 2015

Table 4. Comparison between the adjusted EC coarse emission simulation and original one.

	Adjusted EC coarse fraction			Original (Nordmann et. al., 2014)			
Sites	MB	MNB	R^2	MB	MNB	R^2	Air mass
Bösel	0.12	0.13	0.81	−0.31	−0.21	0.61	East
Leipzig-TROPOS	−1.01	−0.47	0.69	−1.57	−0.7	0.35	East
Hohenpeißenberg	−0.52	−0.64	0.43	−0.59	−0.72	0.66	Southeast
Zugspitze	−0.22	−0.56	0.72	−0.26	−0.46	0.79	Southeast

ACPD
15, 31053–31087, 2015

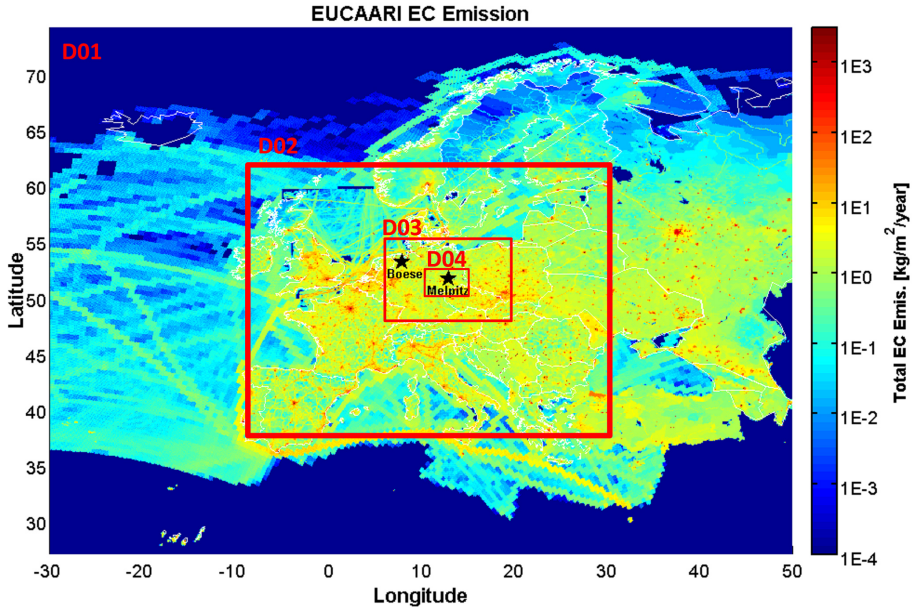

Figure 1. EUCARRI (resolution 7 km) EC emission (kg m^{-2} year^{-1}). The 4 nested model domains (D01-D04) are indicated in the picture. Melpitz and Bösel (Boesel) are marked by black stars.

ACPD
15, 31053–31087, 2015

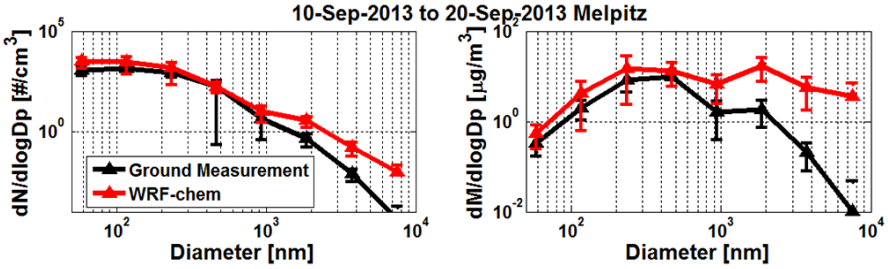

Figure 2. Comparison of Particle Number Size Distribution (PNSD, left) and Particle Mass Size Distribution (PMSD, right) between WRF-Chem model and Melpitz measurements. Model results indicated by the red lines and measurements by the black lines. The size distributions are averaged in the period 10–20 September 2013, the error bar indicate the upper and lower limits.

ACPD
15, 31053–31087, 2015

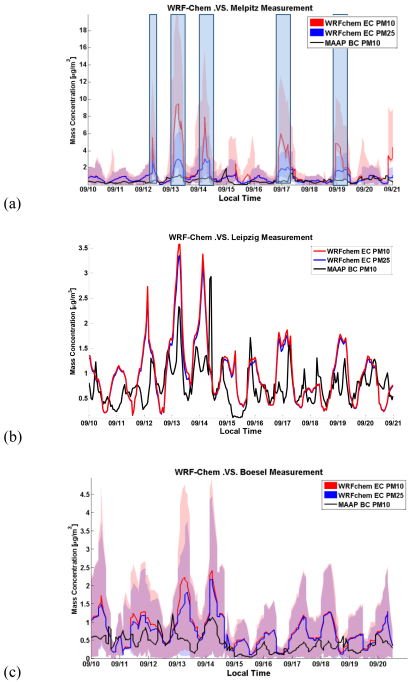

Figure 3. The comparison ofr EC/BC concentration between model and MAAP measurements. Red line: EC concentration in PM_{10} of model result; blue line: EC concentration in $PM_{2.5}$ of model result; black line: BC concentration in PM_{10} of MAAP measurement, used as the best approximation of EC. The shaded areas indicate the model uncertainty defined by the maxima (upper limit of the shade) and minima (lower limit of the shade) values within 12 km distance from Melpitz/Bösel. The blue rectangles mark the EC plume episodes at Melpitz. **(a)** Melpitz: modelling result derived from D04 simulation with 2 km resolution; **(b)** Leipzig-TROPOS: modelling result derived from D04 simulation with 2 km resolution; **(c)** Bösel: modelling result derived from D03 simulation with 6 km resolution.

ACPD
15, 31053–31087, 2015

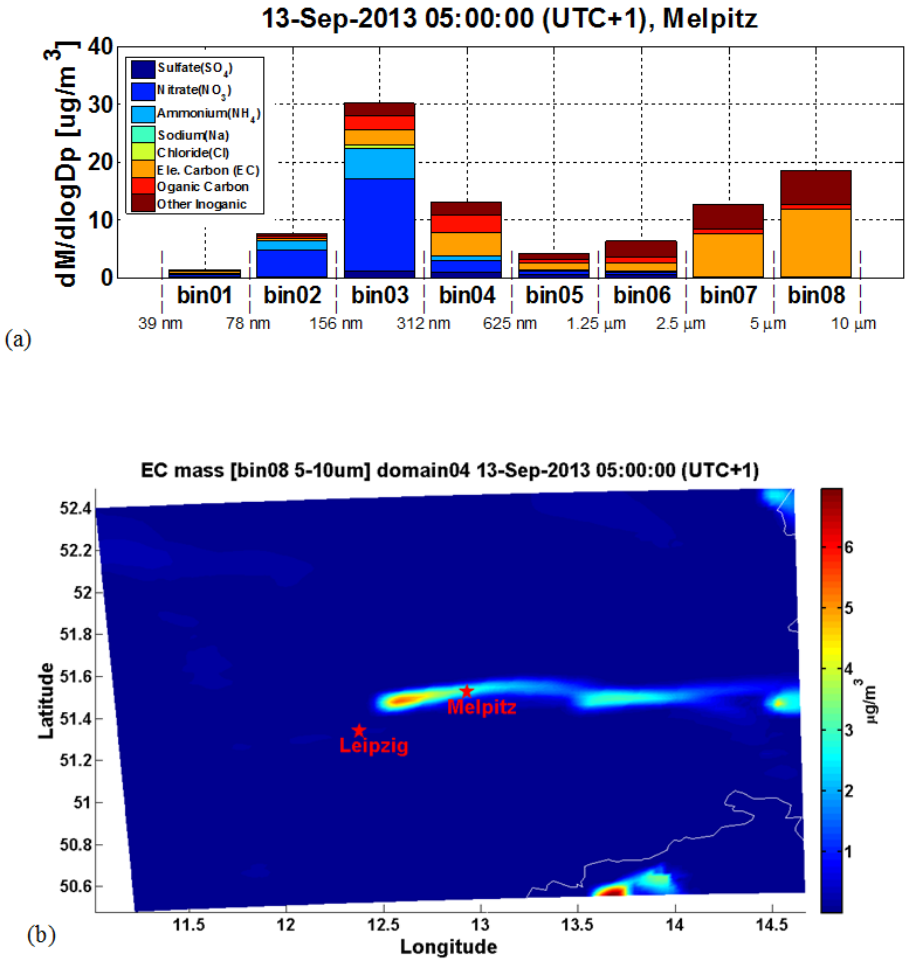

Figure 4. The model result: **(a)** aerosol chemistry compounds for each bins of Melpitz; **(b)** horizontal distribution of EC in bin08 (5–10 µm) at 05:00 (UTC + 1) of 13 September 2013.

ACPD
15, 31053–31087, 2015

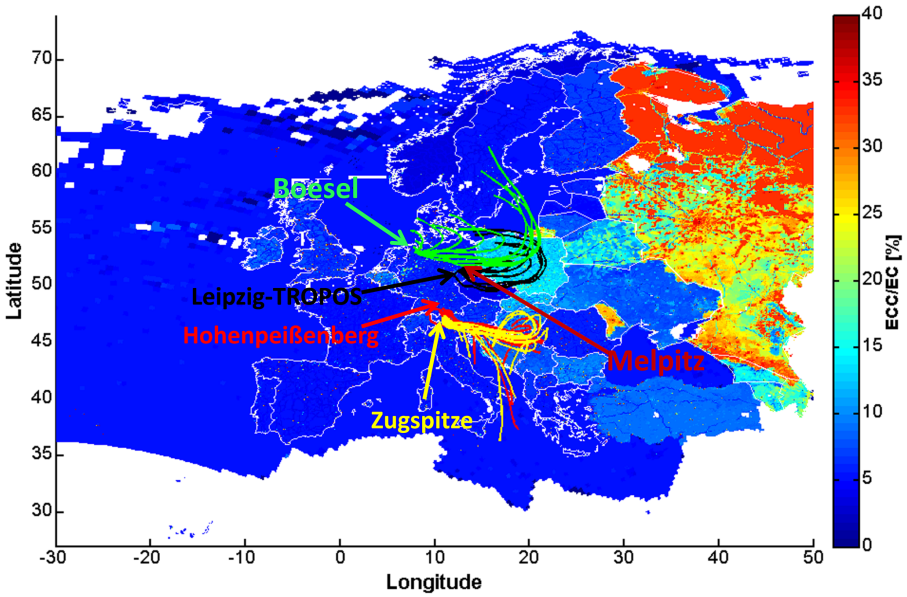

Figure 5. EUCAARI EC emission coarse mode fraction. The location of Bösel, Leipzig-TROPOS, Melpitz, Hohenpeißenberg and Zugspitze are marked in the map. The colored lines indicated the 3-days back trajectories for each site (without Melpitz), in the period from 1 to 4 April 2009 with 6 h interval.

ACPD
15, 31053–31087, 2015

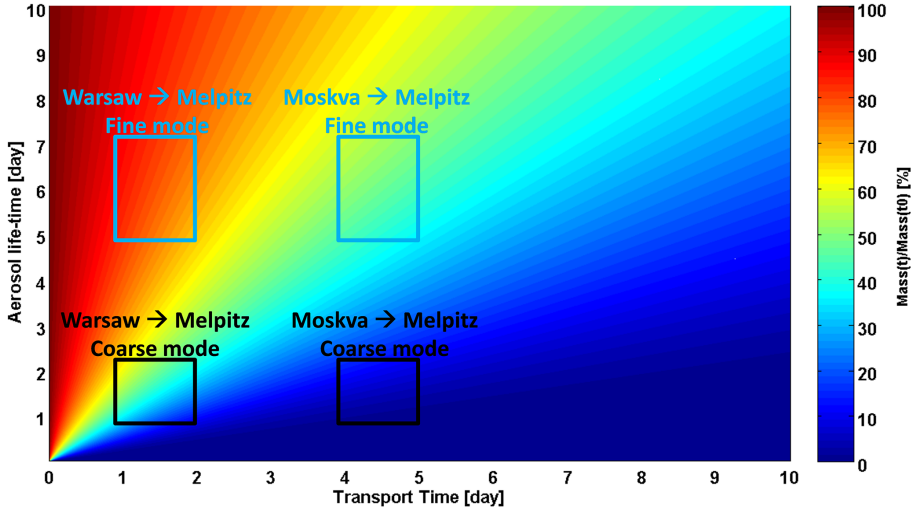

Figure 6. Aerosol mass residential rate with relationship of transport time and lifetime. The color indicates the percentage of aerosol mass that can be transported to Melpitz.

ACPD
15, 31053–31087, 2015